electronics

MDPI

Article

An Adaptive Protection Scheme for Coordination of Distance and Directional Overcurrent Relays in Distribution Systems Based on a Modified School-Based Optimizer

Mohamed Abdelhamid [1], Salah Kamel [1], Ahmed Korashy [1], Marcos Tostado-Véliz [2,*], Fahd A Banakhr [3] and Mohamed I. Mosaad [3]

[1] Department of Electrical Engineering, Faculty of Energy Engineering, Aswan University, Aswan 81528, Egypt; mohammed.abdulhameed@aswu.edu.eg (M.A.); skamel@aswu.edu.eg (S.K.); ahmed.korashy2010@yahoo.com (A.K.)
[2] Electrical Engineering Department, University of Jaen, EPS, 23700 Linares, Spain
[3] Electrical and Electronic Engineering Technology Department, Yanbu Industrial College, Yanbu Al Sinaiyah, Yanbu 46452, Saudi Arabia; banakherf@rcyci.edu.sa (F.A.B.); habibm@rcyci.edu.sa (M.I.M.)
* Correspondence: mtostado@ujaen.es

Abstract: This paper presents an adaptive protection scheme (APS) for solving the coordination problem that deals with coordination directional overcurrent relays (DOCRs) and distance relays second zone time, in relation to coordination with DOCRs. The coordination problem becomes more complex with the impact of renewable energy sources (RES) when added to the distribution grid. This leads to a change in the grid topology, caused by the on/off states of the distribution generators (DG). The frequency of topological changes in distribution grids poses a challenge to the power system's protection components. The change in the state of DGs leads to malfunction in reliability and miscoordination between protection relays, since that causes a direct effect to the short circuit currents. This paper used the school-based optimization (SBO) algorithm, which simulates the educational process, in order to deal with coordination problems. That algorithm is modified (MSBO) by modified both learning and teaching processes. The IEEE 8-bus test system and IEEE 14-bus distribution network are used to validate the proposed coordination system's effectiveness when dealing with the coordination process between distance and DOCRs, at both the near- and far-end in the typical topological grid and with DGs in working order.

Keywords: power system protection; overcurrent relays; protection relays; metaheuristic; school-based optimizer

Citation: Abdelhamid, M.; Kamel, S.; Korashy, A.; Tostado-Véliz, M.; Banakhr, F.A.; Mosaad, M.I. An Adaptive Protection Scheme for Coordination of Distance and Directional Overcurrent Relays in Distribution Systems Based on a Modified School-Based Optimizer. *Electronics* **2021**, *10*, 2628. https://doi.org/10.3390/electronics10212628

Academic Editors: Marinko Barukčić, Nebojša Raičević and Vasilija Šarac

Received: 9 September 2021
Accepted: 19 October 2021
Published: 27 October 2021

1. Introduction

Nowadays, the protection field is one of the more indexing issues in power systems. Directional overcurrent relays (DOCRs) and distance relays are both commonly used for protecting transmission lines. These protection devices monitor the transmission lines from both ends of the lines for faults that cause trip scenarios to be activated.

Overcurrent relays (OCRs) generally work by the magnitude of the fault current, which is set inside relay's parameters, while in DOCRs, adding the direction of the passing current through transmission lines. This direction is determined by voltage phasor from the potential transformer. So, DOCRs are more expensive than normal OCRs but more effective than OCRs. These relays must be operating in the backup case, with a delay time higher than the primary relay [1].

The second protection is distance relays, which have two main zones. The first one works immediately after fault detection. This zone covers 80% of the transmission line to ignore calculation errors. Then, the second zone covers up to 120% of the transmission line by delay time; this wide area covers a part of another transmission line [2].

The main problem in this paper regards reducing the protection relay's operation times, to provide the ability for protection devices to isolate the fault area. This saves the lifetime of power system components, and the power system becomes healthier and more reliable. However, the coordination problem of DOCRs and distance relays is more complex and highly constrained, owing to constraints between DOCRs pairs and DOCRs and distance relays pairs. The miscoordination of these protection relays overlap protection operates and does not utilize the advantages of both distance and DOCRs relays [3,4].

The impact of RES-based DGs adds to the distribution system. RES, such as solar energy and wind energy sources, are integrated with the power system. DGs and the coordination problem present many challenges, such as the change of fault current magnitude and flow of direction [5].

This coordination challenge, which is the result of DGs, needs a flexible structure. This paper discussed adaptive protection systems (APS), in order to solve this protection coordination problem. APS gives the ability to change relays settings for both DOCRs and distance relays, according to change in network states, based on the DG's on/off states, using predetermined settings. APS was tested with various scenarios, which are probably tripped in-network, and the optimal settings for protection relays in each scenario were determined. This gives the protection system the ability to minimize miscoordination and malfunction. The main advantage of APS is making the protection system more selective and reliable than conventional or fixed systems [6]. APS's settings group of protection relays is determined by computing optimal settings using an optimization algorithm for each scenario, which is based on the DG's states [7].

In recent years, many optimization algorithms are used for solving coordination problems in literature, of DOCRs coordination, such as the particle swarm optimizer (PSO) and modified PSO in [8], genetic algorithm (GA) and hybrid GA in [9], biogeography-based optimization algorithms (BBO) in [10], differential evolution algorithm (DE) and trigonometric DE algorithm (Tri-DE) in [11], firefly algorithm (FA) and improved FA (IFA) in [12], hybridized whale optimization algorithm (WOA), and hybridized WOA in [13], Jaya Algorithm and oppositional Jaya algorithm (OJaya) in [14], moth–flame optimization (MFO) and improved MFO (IMFO) in [15], political optimization algorithm (PO) in [1], artificial optimizing algorithm(AEO) in [16], and evaporation rate water cycle algorithm in [17].

Then, for the coordination of both the DOCRs and distance, such as the genetic algorithm (GA) in [18,19], water cycle algorithm (WCA) [19], Jaya optimization algorithm [20], grey wolf optimization (GWO) [19], ant colony optimization (ACO), and hybrid ACO algorithm in [21].

The adaptive protection scheme is important for coordinating the protection relays, in order to deal with the change in topology of the distribution network, which results from the DG's on/off status. This topological change causes a change in the short-circuit current. Hence, modern protection systems, which deal with DGs or RES, are needed for an adaptive scheme.

APS is basically dependent on the communication network between the smart grid's components, as a part of information and communication technologies (ICT), or it is dependent on SCADA. These communication networks give APS the ability to set relays remotely.

Because of the real-time performance of the revolution of optimization algorithms (in terms of millisecond or microseconds), as well as high computerized performance, in many research papers, APS is shown to be dependent on the optimization algorithms to coordinate DOCRs, such as using the: particle swarm optimization (PSO) in [22], genetic algorithm (GA) in [23], differential evolution algorithm (DEA) in [24], ant colony optimization (ACO) [25], gravitational search algorithm (GSA) in [26], firefly algorithm (FA) in [27], manta ray foraging optimization (MRFO) in [7], and hybrid Harris hawks optimization (HHO) in [28].

Metaheuristic optimization algorithms usually generate random initial values, as its population within search space limiters then improves the population fitness within a systematic process. The standard of metaheuristic optimization algorithms is always

formed by intrapopulation collaboration. The original SBO algorithm utilized subgroups of the parallel populations, with independent values that collaborate. Increase the capability of exploration of the algorithm and improve the overall efficiency. SBO is a collaborative, multi-population framework utilized by TLBO. This algorithm used two stages: the first stage is about a series of metaheuristics works, independent for exploring the different areas of the search space. Then, the second stage concentrated the search on the sub-region within the best solutions. This type of algorithm has many challenges; one of them is selecting and implementing the first stage termination criterion. The terminal criterion introduces parameters that need to be tuned for a specific problem [29].

SBO extends the basic model of TLBO, with both learning and teaching phases; however, MSBO used TLBO with a modified learning phase. Then, teachers can be rearranged with a roulette wheel role to other classrooms to share their knowledge; while, MSBO used multiple teachers for each classroom to improve share knowledge processes between classrooms and increased the exploitation of the population into the teaching phase [30].

SBO is applied to solve many other engineering optimization problems, such as steel frame design in [29,31] and solar cell parameters estimation in [32]. SBO is effective in solving these optimization problems.

Other methods are suggested to deal with APS, such as multi-agents in [33,34] and Q-learning with an environment APS in [35].

Contributions of this paper are as follows:

- An adaptive protection scheme was designed to coordinate both DOCRs and distance relays. This paper is the first one that deals with this problem in APS, as a solution to the DG impact. The effect of distance relays complicates this coordination problem in the DOCR's coordination process, in addition to the impact of DGs.
- The original SBO algorithm was modified to improve the response and convergence of the proposed algorithm. In doing so, two main points were modified, learning and the teacher-selected process. This algorithm could be effective in solving other power systems' important topics, such as load frequency control, parameter estimation of the solar cell, optimal location, and the sizing of DGs.
- The proposed protection system in this paper was tested on both IEEE 8-bus and IEEE 14-bus distribution networks, with the effect of DG's on/off states.

The rest of the paper is as follows: Section 2 is about the mathematical modelling of coordination problems. Section 3 presents the proposed protection scheme. Then, in Section 4, the performance of both SBO and MSBO, for solving the coordination problem in IEEE 8-bus and IEEE 14-bus distribution networks, is presented. Finally, Section 5 shows the conclusions.

2. The Mathematical Modelling of Coordination Problem

The main goal of this paper is to get the optimal coordination of DOCRs and distance relays. The optimal solution to this problem is minimizing the total operation time of DOCRs at both ends of the near-end (*TNR*) and far-end (*TFR*), in addition to the second zone time of distance relays (T_{Z2}). The minimum total operation time is the objective function (*OF*), shown as following [21,36,37]:

$$OF = min\left(\sum_{i=1}^{n} TNR_i + \sum_{i=1}^{n} TFR_i + \sum_{i=1}^{n} T_{Z2}i + F^{Pen}\right), \quad (1)$$

The standard time inverse DOCRs characteristics, depending on the international electrotechnical commission (IEC) standards, are presented by the following equation [16]:

$$T_i = \frac{\propto * TDS_i}{\left(\frac{I_f}{I_{pi}}\right)^{\beta} - \gamma}, \quad (2)$$

where T_i is the operation time of relay at any end of transmission line for i relay, TDS is its time dial setting, and I_p is its pick-up current. The other α, β, and γ are constants with 0.14, 0.02, and 1, respectively [1].

2.1. The Problem's Limiters

The main limiter of any protection relay is the maximum operation time (T_{max}) to prevent bad operation, which saves the power system component's lifetime. That limiter must be lower than 2 s [16].

Any relay settings, in coordination with the problem, have minimum and maximum limiters, as shown in the following equations [21]:

$$TDS_{min} \leq TDS \leq TDS_{max}, \tag{3}$$

$$Ip_{min} \leq Ip \leq Ip_{max}, \tag{4}$$

$$Tz2_{min} \leq Tz2 \leq Tz2_{max}, \tag{5}$$

2.2. The Problem's Constraints

The proposed optimization problem becomes a higher constraint problem, via the constraints between the primary and backup pair of DOCRs, in addition to the relationship between the DOCRs, distance, and pairs relay at both ends (near and far). Those constraints are used to avoid miscoordination, which may happen during faults between protection relays.

The relationship between DOCRs pair relays, at any end, as shown in Figure 1, must deal with the backup relay (t_b), operated with a delay on the primary relay (t_p). This delay time is called coordination time interval (CTI). The value of CTI is determined according to the type of protection relays. For electromagnetic relays, the CTI value must be more than 0.3 s, while, in the case of digital relays, more than 0.2 s; the digital relays are used in this paper [38]. The following equation shows these constraints [21]:

$$t_b{}^{f1} - t_p{}^{f1} > CTI, \tag{6}$$

$$t_b{}^{f2} - t_p{}^{f2} > CTI, \tag{7}$$

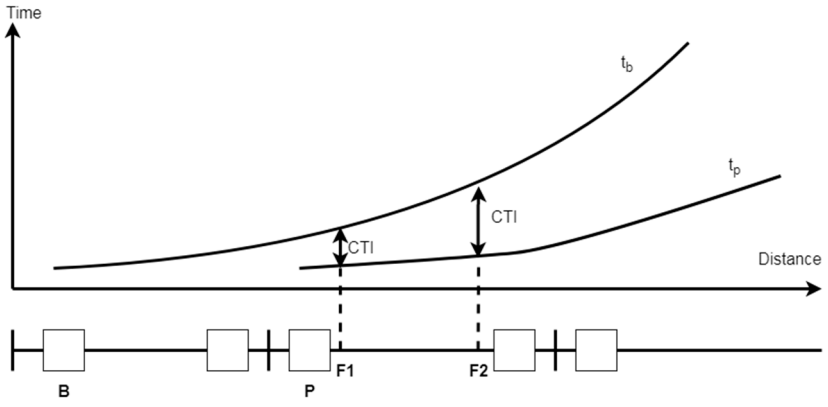

Figure 1. The relationship between primary and backup DOCRs.

The relationship between DOCRs and distance pair relays is shown in Figure 2. The backup distance relay aliasing, with the primary DOCRs relay at the near end, and T_{Z2b} must delay on $t_p{}^{f1}$, with the CTI as described in Equation (8); Equation (9) describes the relationship between distance and DOCRs at the far end. At the far end, the second zone of primary distance relay (T_{Z2p}) must delay on primary DOCRs operation time $\left(t_p{}^{f1}\right)$ with CTI [21].

$$T_{Z2b} - t_p{}^{f1} > CTI, \tag{8}$$

$$T_{Z2p} - {t_p}^{f2} > CTI, \tag{9}$$

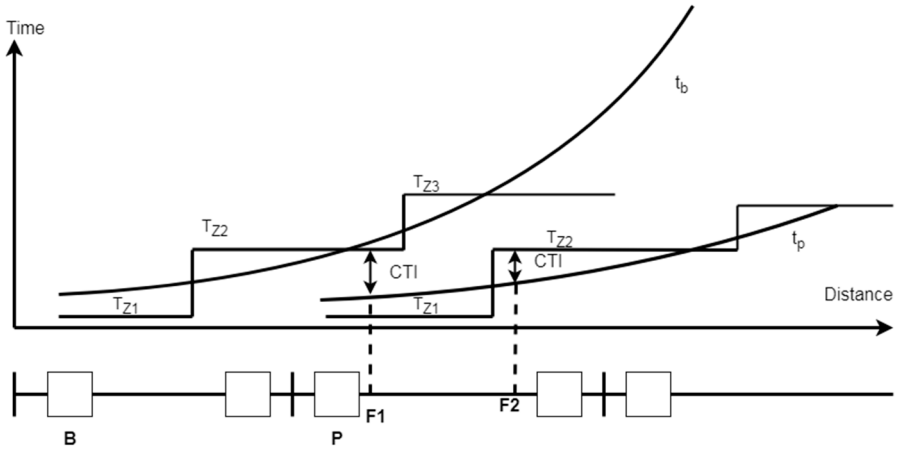

Figure 2. The relationship between DOCRs and Distance pair relays.

This relationship was developed to specify the minimum value of the second zone of the distance relay, based on the operation time of the primary relay at both ends near and far. This idea is discussed in [39]. Equations (8) and (9) are rearranged to Equations (10) and (11). Then, the maximum value of these equations is used as the specific second zone of distance relay's time. This point helps to reduce the penalty and constraints.

$$T_{Z2b} = {t_p}^{f1} + CTI, \tag{10}$$

$$T_{Z2p} = {t_p}^{f2} + CTI, \tag{11}$$

$$T_{Z2} = max\left(T_{Z2b}, T_{Z2p}\right), \tag{12}$$

The penalty function is recommended for use in the main goal of eliminating miscoordinations, as in the following equation [40]:

$$F^{pen} = \mu * \begin{cases} 1\ if\ T^{backup} - T^{primary} < CTI \\ 0\ if\ T^{backup} - T^{primary} \geq CTI \end{cases}, \tag{13}$$

When miscoordination occurs in this penalty function, F^{pen} increases the total time of OF. As a result, the optimization algorithm attempts to eliminate miscoordination, in order to reduce the size of OF; μ is the weighting factor in this penalty function [37].

3. The Proposed Protection Scheme

3.1. Smart Grid and Adaptive Protection Scheme (APS)

In this research work, the proposed scheme is based on optimization solutions by an optimization technique. In this paper, the school-based optimization algorithm, used to evaluate the optimization solutions, in addition to this paper, included modifications for that algorithm, in order to improve its convergence characteristics and ability to find better optimization solution, as described in the next section.

The flow diagram (Figure 3) presents APS, considering DG's impact. The centralized processing server is used to optimize SCADA data. These data will be generated by APS-proposed algorithms, for resetting the DOCRs and distance relays. The following steps refer to the main points of the proposed APS flow chart.

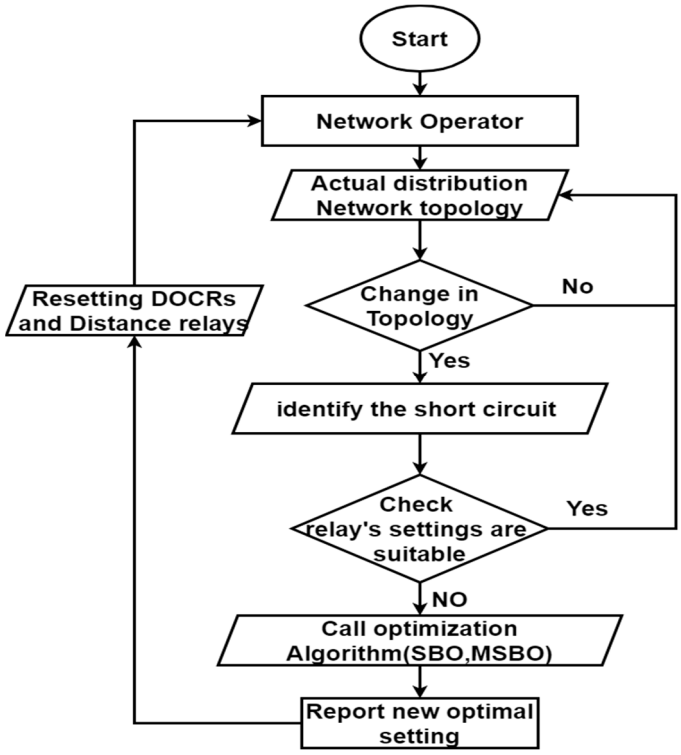

Figure 3. Flow diagram of APS.

The first point determined the actual distribution network topology, especially the state, location, and size of the DGs. Check for a change of distribution network topology. In case of no change, the APS stays with the current protection relay's settings; in the case of a change in topology, the APS moves to the next point.

In the second point, APS identifies the short current through CBs, ETAP was used in this paper for this mission. Then, check the ability of the current relay's settings, in order to save the protection system without loss-coordination of protection relays or miscoordination between protection relays. In case of the ability of the current setting to protect the distribution network, the APS returns to the previous point. However, it will move to the next point in the case that the relay's setting misses their job to protect the distribution network.

In the third point, APS calls the proposed optimized algorithm. Then, the algorithm searches for optimal solutions that are suitable to cover the changes in the distribution network, without miscoordination or loss-coordination. Finally, the APS reports the optimal solution of protection relay's settings and sends them through ICT and in-distribution network update IEDs. APS will stick to new changes in the distribution network [41].

3.2. Original School-Based Optimization Algorithm

SBO is a metaheuristic algorithm, as shown in its flowchart in Figure 4. SBO is formed from many classrooms and has many teachers. Each classroom used the TLBO algorithm, in order to be built. Each classroom has a teacher, which is the population with the best fitness. Teachers are joining to a pool of teachers. In this pool, teachers are distributed by a roulette wheel to a new classroom, in order to transfer the knowledge between them.

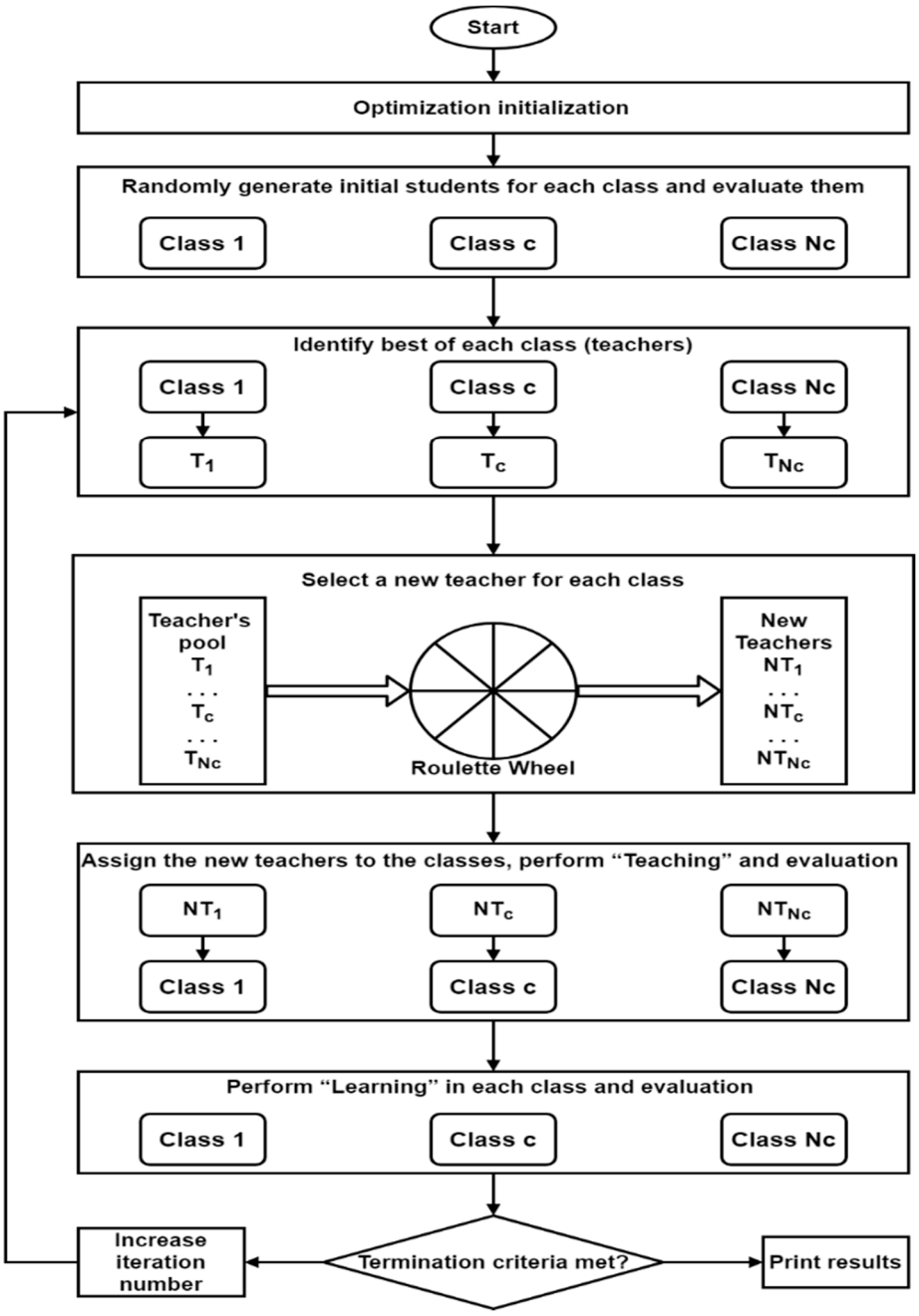

Figure 4. Flow chart of SBO algorithm.

The TLBO algorithm was inspired by the educational process in the classroom. That algorithm has two main phases. These phases are about the educational process and exchanging knowledge. The first phase is called the teacher phase. In this phase, the knowledge is transferred from teacher to students. The other phase is called the learning phase. That phase simulates the cooperative learning between students [29].

3.2.1. Teaching Phase

In this phase, the optimization algorithm simulates the teaching process to students who are trying to update themselves by knowledge transfer from their teacher. That representation is mathematically as follows:

$$X^k_{new}(j) = X^k_{old}(j) \pm \Delta(j)\,, \tag{14}$$

$$\Delta(j) = T_F \times r|M(j) - T(j)|, \tag{15}$$

where $X^k(j)$ refers to the solution as a student with index jth, $\Delta(j)$ is the difference between the teacher and the mean of the class, T_F is a teaching factor and equal to 2, r is a random value between [0, 1], $T(j)$ is the solution as a teacher, and $M(j)$ is the mean of the classroom and is represented as follows [30]:

$$M(j) = \frac{1}{N}\sum_{k=1}^{N} X^k(j), \tag{16}$$

$$M(j) = \frac{\sum_{k=1}^{N} \frac{X^k(j)}{F^k}}{\sum_{k=1}^{N} \frac{1}{F^k}}, \tag{17}$$

where N is the population. F^k is the penalized fitness of student solution with indexing kth.

Equation (17) is about the fitness-based mean. This formula gives more emphasis to students and improves the performance of the TLBO algorithm [42].

At the end of the iteration, the solution that has the best fitness is chosen as a new teacher in the next iteration.

3.2.2. Learning Phase

Interactive learning between students in each classroom can develop the student's performance then develop the performance of the classroom. The learning phase is given by following steps:

1. Randomly selected student p and another q while $p \neq q$.
2. If the fitness of student p is better than student q.

$$X^p_{new}(j) = X^p_{old}(j) + r\left[X^p_{old}(j) - X^q(j)\right], \tag{18}$$

Otherwise,

$$X^p_{new}(j) = X^p_{old}(j) + r\left[X^q(j) - X^p_{old}(j)\right], \tag{19}$$

where r is a random number between [0, 1].

This phase moves student p towards student q if student q has a better solution; while, if student p has a better solution, it will move away from student q [42].

3.3. Modified SBO Algorithm

The original SBO algorithm was modified, as shown in its flowchart in Figure 5. That is based on two main points, in order to improve its ability to explore and exploit in the original algorithm. The first point is about the learning phase, which was discussed in the previous section. This part is modified by changing the techniques of learning between students by three additional steps, discussed below. The second point is to select more than one teacher, via a roulette wheel, in order to speed the process up and obtain a better knowledge transfer process inside the class (and with other classes).

3.3.1. First Point: A Modified Learning Phase

This point has been modified to exploit students in each classroom to reach new points within a limited search area that has better fitness values, by using the following steps:

1. This step does not choose the student p randomly but as the place in the classroom.
2. The student q is chosen randomly but not repeated with another student and cannot be equal to student p.
3. Equations (18) and (19) are both applied and choosing the best value to compare with the student p fitness value (to replace or not).

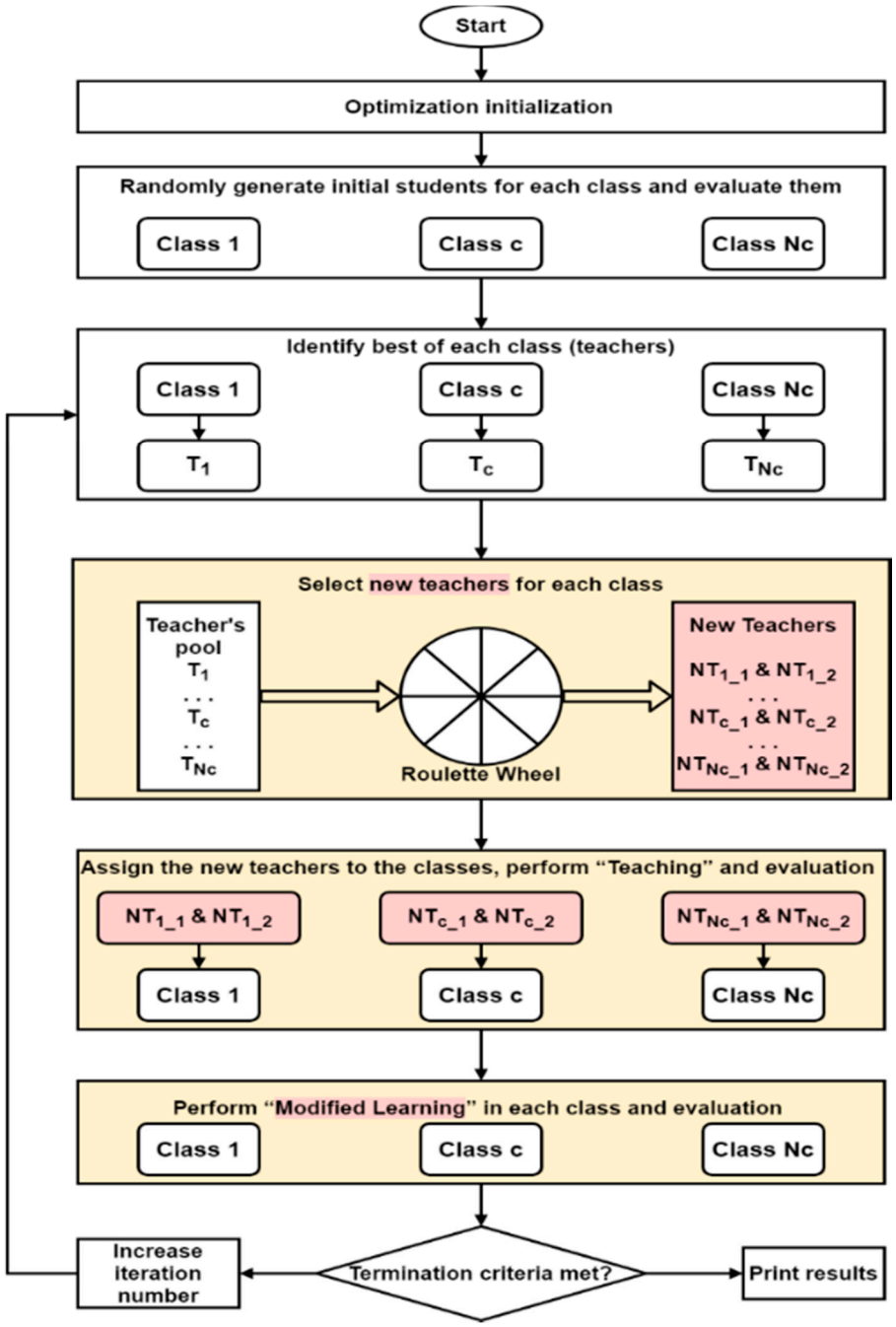

Figure 5. Flow chart of MSBO algorithm.

3.3.2. Second Point: Teacher Selected

The original algorithm selected one teacher, but the improved algorithm selected more than one. This point increased the knowledge transfer process between classrooms. In the original algorithm selected, one teacher from another classrooms carried knowledge from it; however, after that, each classroom takes knowledge from many classrooms and then selected new points after evaluating the fitness values, in order to accept the best fitness value between new points affected by teachers. This improved the teacher phase's equation used previously but repeated with each teacher. Teachers were distributed to classrooms by roulette wheel and this modified was used, too, but selected many teachers for each classroom. The number of teachers for each classroom was selected by users and, in this paper, double teachers were selected.

4. Results and Discussion

The optimization setting of TDS, IP, and TZ2 were tuned by the MATLAB program, used for both SBO and MSBO to solve the optimization problem. These algorithms, discussed in previous sections, used population, classrooms, and maximum iterations, with values are 300, 25, and 1000, respectively. The algorithms were successfully tested in coordination tested systems, i.e., the IEEE 8-bus test system and the IEEE 14-bus distribution network. Each test system has two varying cases: the first is the normal topological grid and the second is after added external power generation for the original grid.

The optimum settings were used to calculate the operation time of the primary and backup protection relays at the near-end and the far-end. These points were tested to succeed in the optimal solution, in order to pass system constraints. The protection devices, assumed with digital relays and CTI, must be greater than or equal to 0.2 s. Relays with normal characteristics constants are α, β, and γ, with values of 0.14, 0.02, and 1.0, respectively, maximum and minimum TDS values of 1.1 s and 0.1 s, respectively, maximum and minimum PS were 4 and 0.5, respectively, and the maximum time for operating the primary DOCRs or distance relays was 1.5 s [21].

MATLAB R2016a was used on a computer with a CPU of 1.70 GHz processor and 4 GB DDR3 RAM, for tuned optimum settings, while ETAP 12.6.0 was used for the calculation three phase fault currents.

4.1. Test System I: IEEE 8-Bus Test System

The APS was tested on the IEEE 8-bus test system, as shown in Figure 6, for the original topological system, with an external grid linked in bus number 4. This system consists of 8 buses, which are connected with 7 lines and used 14 relays on the ends of the lines to protect these transmission lines. This system has two synchronous generators to feed 4 loads, in addition to the 400 MW for external grid entry and out-of-work [21,43].

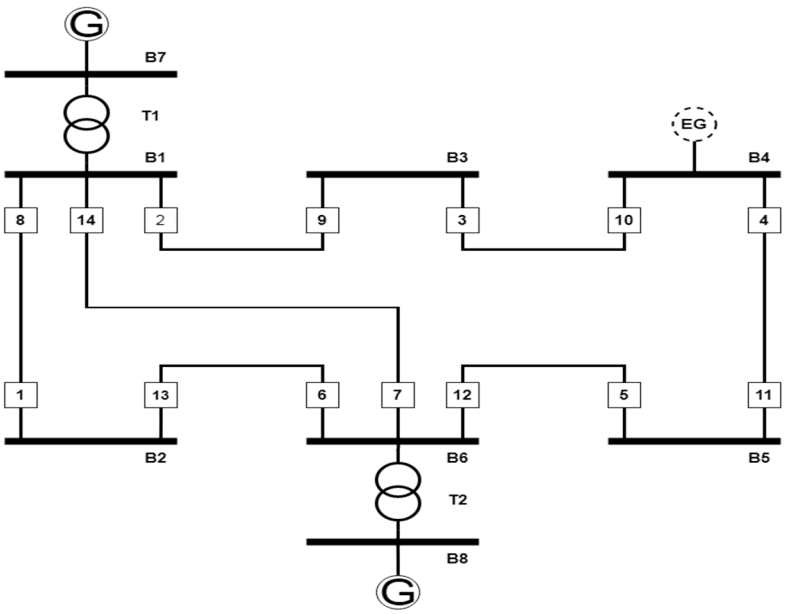

Figure 6. The single line diagram of IEEE 8-Bus.

This was a highly constrained, nonlinear optimization problem. It had 42 variables of design, which were tuned by optimization algorithms, in each case. The optimal solution was limited with minimum and maximum TDS, IP, TZ2, and T operate limiters. Additionally, they were constrained with a CTI value between the operation time of pairs primary and backup constraints. These constraints were 32 between DOCRs and equal to 40 between DOCRS and distance relays in the normal grid, while the external grid, on

the state the constraints, became 34 between DOCRS and was still equal to 40 between the DOCRs and distance relays.

The ETAP program used to calculate three-phase fault currents is presented as Appendix A Table A1 for the normal grid. Additionally, for the second case, data was extracted from [43].

Table 1 lists the optimal settings for protection relays using both SBO and MSBO in normal topological settings, and the external grid is on. This table proved the MSBO has optimum solutions that are better than the optimum solution of SBO.

Table 1. IEEE 8-bus's relays setting.

Relay	Normal Topological Grid						With External DG					
	Original SBO			Modified SBO			Original SBO			Modified SBO		
	TDS	IP	TZ2	TDS	IP	TZ2	TDS	IP	TZ2	TDS	IP	TZ2
1	0.194	174.94	1.07	0.164	191.56	0.984	0.193	229.12	1.108	0.119	370.20	1.037
2	0.287	289.93	1	0.198	528.22	0.936	0.274	353.42	1.013	0.168	723.15	0.928
3	0.332	80.55	0.875	0.252	137.37	0.815	0.236	242.43	0.928	0.143	549.25	0.903
4	0.125	318.77	0.793	0.128	249.02	0.719	0.173	393.64	0.86	0.158	438.72	0.84
5	0.1	235.55	1.425	0.1	158.21	0.917	0.114	434.09	0.974	0.1	500.20	0.993
6	0.175	654.44	1.049	0.286	120.14	0.823	0.216	389.94	0.9	0.297	140.18	0.843
7	0.297	147.82	1.068	0.208	247.29	0.982	0.205	443.09	1.174	0.369	80.03	0.991
8	0.257	226.38	0.931	0.128	725.52	0.916	0.303	420.07	1.258	0.269	205.83	0.884
9	0.1	173.26	0.994	0.1	145.66	0.861	0.314	127.59	1.174	0.256	143.03	1.039
10	0.136	389.05	0.913	0.155	171.41	0.698	0.227	455.43	1.121	0.177	552.63	1.012
11	0.274	196.10	0.954	0.123	578.75	0.805	0.147	784.60	1.13	0.154	666.46	1.049
12	0.382	167.49	1.053	0.166	631.70	0.869	0.227	595.26	1.052	0.317	295.35	1.055
13	0.198	191.93	1.146	0.226	120.34	1.011	0.165	271.95	1.088	0.167	284.74	1.127
14	0.233	282.76	1.147	0.128	460.94	0.935	0.264	243.24	1.089	0.321	173.52	1.123
OF		33.705			28.072			35.388			32.601	

The normal case of the IEEE 8-bus test system constraints, which occur by optimum solution, was tabulated in Table 2. This table is for primary and backup operation time of DOCRs pairs relay in both near- and far-end. Addition to for constraints between DOCRs and distance relays. Table 3 has the same description as previous Table 2 but deal with another case in which the network is linked with the external grid. These tables show that modified algorithm satisfied all constraints.

Table 2. IEEE 8-bus's operation times of Relay's pairs in normal grid by MSBO.

Pair	Near-End						Far-End					
	DOCRs			D&DOCR			DOCRs			D&DOCR		
	T_p	T_b	CTI	T_p	T_{Z2B}	CTI	T_p	T_b	CTI	T_p	T_{Z2P}	CTI
1	0.423	0.623	0.200	0.423	0.823	0.400	0.784	1.027	0.243	0.784	0.984	0.2
2	0.582	0.784	0.202	0.582	0.984	0.402	0.736	2.390	1.655	0.736	0.936	0.2
3	0.582	0.782	0.200	0.582	0.982	0.400	0.736	1.674	0.939	0.736	0.936	0.2
4	0.535	0.736	0.200	0.535	0.936	0.400	0.615	0.943	0.329	0.615	0.815	0.2
5	0.399	0.615	0.216	0.399	0.815	0.416	0.519	0.752	0.233	0.519	0.719	0.2
6	0.318	0.519	0.201	0.318	0.719	0.401	0.717	1.738	1.021	0.717	0.917	0.2
7	0.517	0.717	0.201	0.517	0.917	0.401	0.623	——	——	0.623	0.823	0.2
8	0.517	0.735	0.218	0.517	0.935	0.418	0.623	——	——	0.623	0.823	0.2
9	0.497	0.717	0.220	0.497	0.917	0.420	0.782	——	——	0.782	0.982	0.2
10	0.497	0.811	0.314	0.497	1.011	0.514	0.782	——	——	0.782	0.982	0.2
11	0.457	0.782	0.325	0.457	0.982	0.525	0.716	——	——	0.716	0.916	0.2
12	0.457	0.661	0.203	0.457	0.861	0.403	0.716	——	——	0.716	0.916	0.2
13	0.298	0.498	0.200	0.298	0.698	0.400	0.661	1.216	0.555	0.661	0.861	0.2
14	0.405	0.605	0.200	0.405	0.805	0.400	0.498	0.924	0.426	0.498	0.698	0.2
15	0.469	0.669	0.200	0.469	0.869	0.400	0.605	0.877	0.272	0.605	0.805	0.2
16	0.532	0.811	0.280	0.532	1.011	0.480	0.669	1.471	0.802	0.669	0.869	0.2
17	0.532	0.735	0.203	0.532	0.935	0.403	0.669	2.480	1.811	0.669	0.869	0.2
18	0.504	0.716	0.212	0.504	0.916	0.412	0.811	7.976	7.165	0.811	1.011	0.2
19	0.394	0.784	0.389	0.394	0.984	0.589	0.735	——	——	0.735	0.935	0.2
20	0.394	0.661	0.266	0.394	0.861	0.466	0.735	——	——	0.735	0.935	0.2

Table 3. IEEE 8-bus's operation times of relay's pairs in case with extrnal grid by MSBO.

Pair	Near-End						Far-End					
	DOCRs			D&DOCR			DOCRs			D&DOCR		
	T_p	T_b	CTI	T_p	T_{Z2B}	CTI′	T_p	T_b	CTI	T_p	T_{Z2P}	CTI′
1	0.378	0.643	0.265	0.378	0.843	0.465	0.837	1.041	0.204	0.837	1.037	0.2
2	0.548	0.839	0.291	0.548	1.037	0.489	0.728	13.984	13.256	0.728	0.928	0.2
3	0.548	0.793	0.244	0.548	0.991	0.443	0.728	1.131	0.404	0.728	0.928	0.2
4	0.527	0.728	0.200	0.527	0.928	0.400	0.703	1.029	0.325	0.703	0.903	0.2
5	0.503	0.703	0.201	0.503	0.903	0.401	0.640	1.537	0.897	0.640	0.840	0.2
6	0.440	0.640	0.200	0.440	0.840	0.400	0.793	1.088	0.295	0.793	0.993	0.2
7	0.531	0.793	0.262	0.531	0.993	0.462	0.643	3.115	2.472	0.643	0.843	0.2
8	0.531	0.923	0.392	0.531	1.123	0.592	0.643	——	——	0.643	0.843	0.2
9	0.593	0.793	0.200	0.593	0.993	0.400	0.791	——	——	0.791	0.991	0.2
10	0.593	0.928	0.335	0.593	1.127	0.534	0.791	——	——	0.791	0.991	0.2
11	0.537	0.793	0.256	0.537	0.991	0.454	0.684	——	——	0.684	0.884	0.2
12	0.537	0.839	0.302	0.537	1.039	0.502	0.684	1.308	0.624	0.684	0.884	0.2
13	0.611	0.812	0.201	0.611	1.012	0.401	0.839	1.656	0.817	0.839	1.039	0.2
14	0.622	0.849	0.227	0.622	1.049	0.427	0.812	2.002	1.190	0.812	1.012	0.2
15	0.619	0.855	0.236	0.619	1.055	0.436	0.849	1.049	0.200	0.849	1.049	0.2
16	0.719	0.928	0.209	0.719	1.127	0.408	0.855	2.770	1.914	0.855	1.055	0.2
17	0.719	0.923	0.204	0.719	1.123	0.404	0.855	1.423	0.568	0.855	1.055	0.2
18	0.485	0.685	0.200	0.485	0.884	0.399	0.927	1.182	0.255	0.927	1.127	0.2
19	0.639	0.839	0.200	0.639	1.037	0.398	0.923	——	——	0.923	1.123	0.2
20	0.639	0.839	0.200	0.639	1.039	0.400	0.923	——	——	0.923	1.123	0.2

The convergence characteristics curves of SBO and MSBO for the normal case and the other case are presented in Figures 7 and 8, respectively. And the penalty occurred by SBO and MSBO during running the optimum algorithm shown in Figure 9. For the normal case while the state of the external grid is shown in Figure 10. These figures showed the convergence of MSBO is better and faster than the original SBO convergence. And the ability of MSBO to avoid penalty and pass constraints quickly.

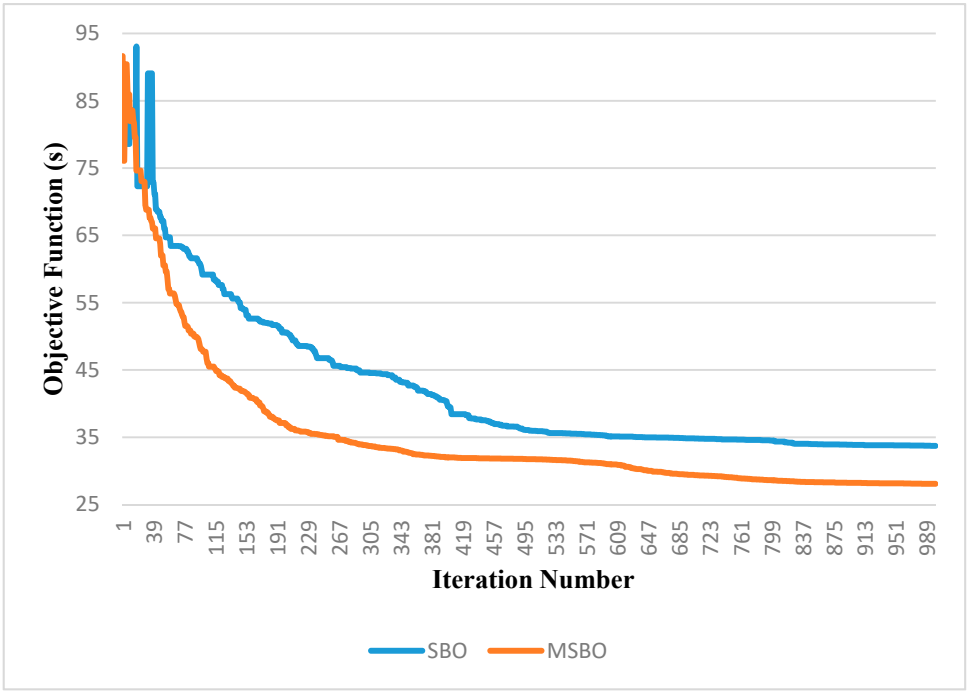

Figure 7. Convergence characteristics of SBO and MSBO in normal case of IEEE 8-bus.

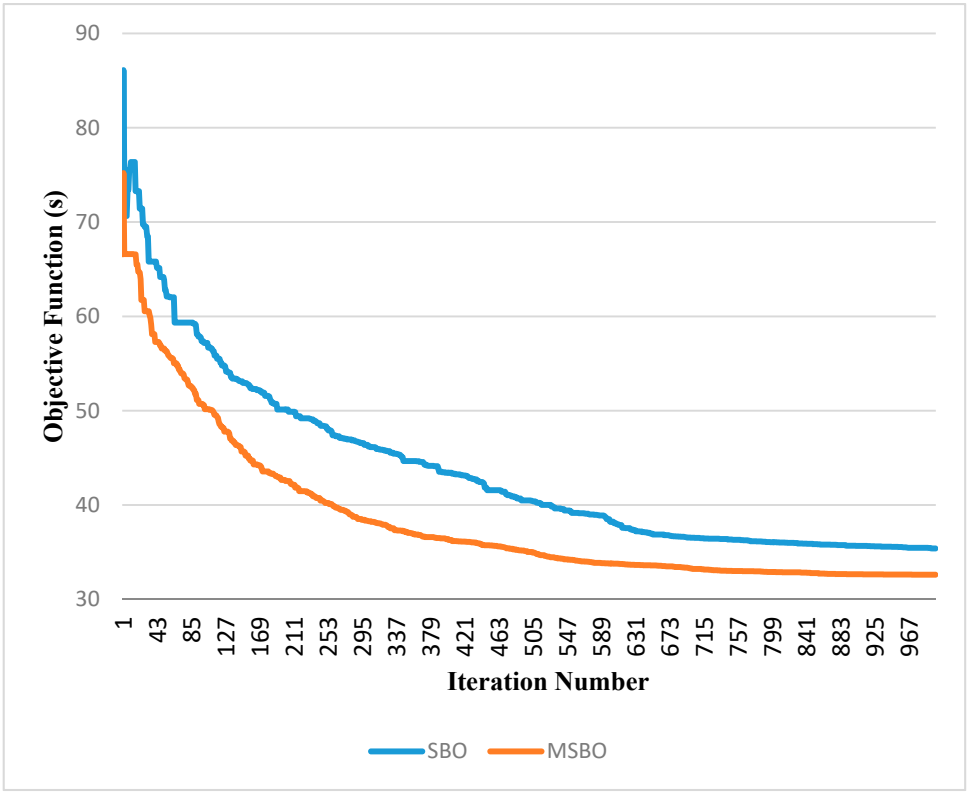

Figure 8. Convergence characteristics of SBO and MSBO in external grid on case of IEEE 8-bus.

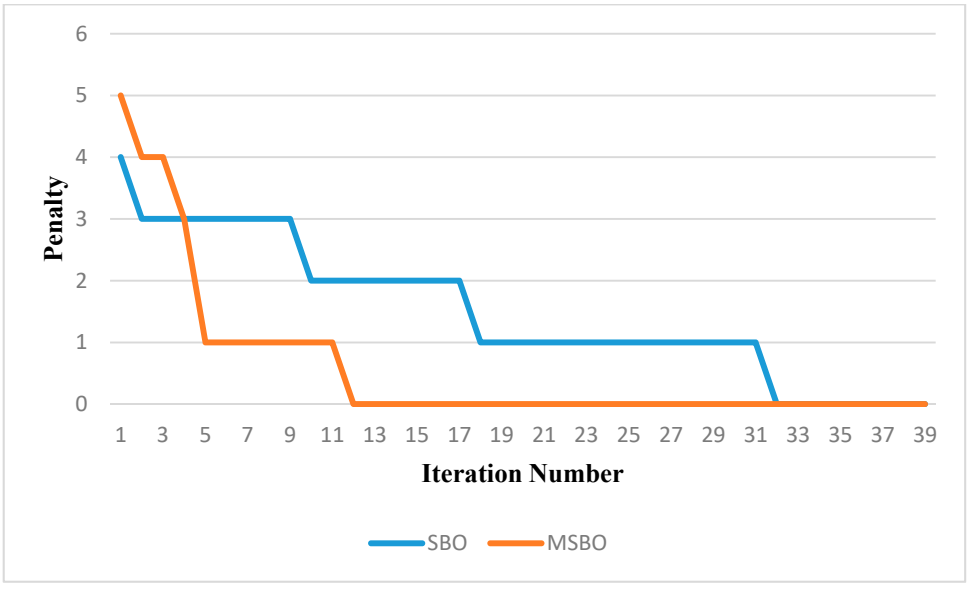

Figure 9. Penalty between SBO and MSBO of IEEE 8-bus test system normal case.

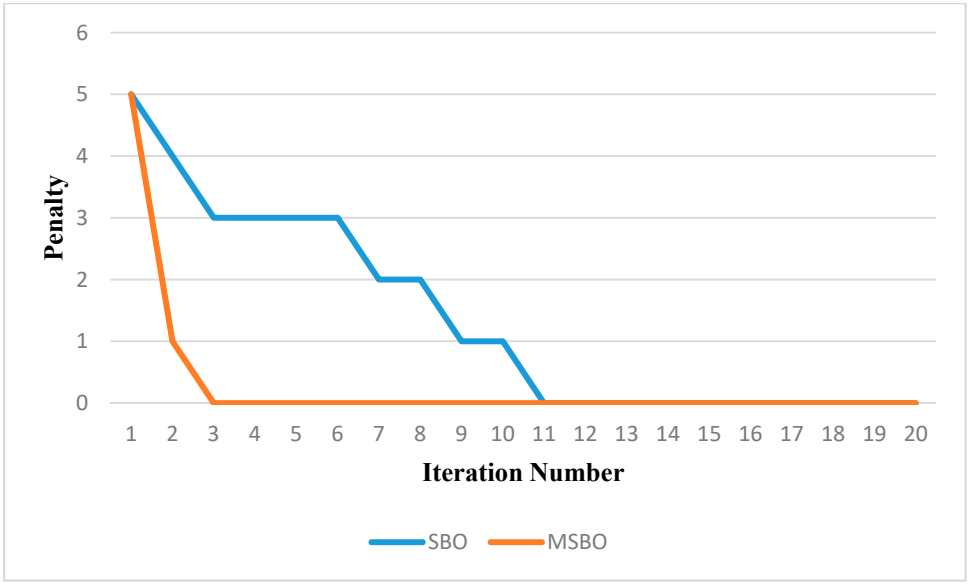

Figure 10. Penalty between SBO and MSBO of IEEE 8-bus test system with external grid on work.

In the normal case, the original SBO has OF with value 33.705 s while MSBO has OF with value 28.072 s and MSBO has 33.705 s after 300 iterations and MSBO passed penalty after 12 iterations while original SBO continuous to iteration 32 to pass system's constraints. For another case, the external grid stat on operation OF becomes 32.601 s and 35.388 s for MSBO and SBO respectively. MSBO reached 35.350 s after 477 iterations. The penalty passed after 11 iterations in the case of SBO while MSBO passed after three iterations. All of these prove the ability of MSBO to increase its exploration and exploitation more than the original algorithm.

4.2. Test System II: IEEE 14-Bus Distribution Network

The IEEE 14-bus distribution network which is shown in Figure 11. Which is a downstream section of IEEE 14-bus. This distribution network has two distribution transformers connected at buses number 1 and 2 to supply it. Each transmission line has a protection relay at every end of the line to form 16 relays [38,44].

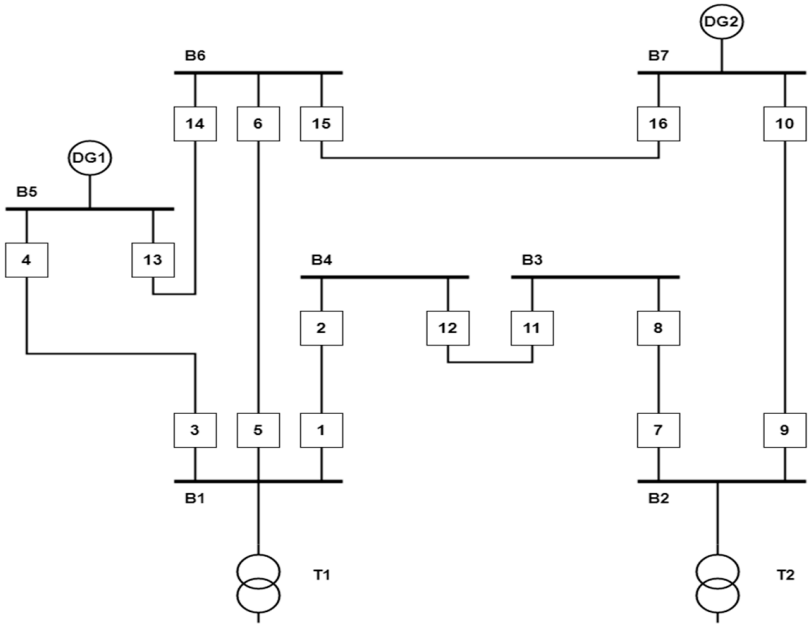

Figure 11. The single line diagram for 14 bus distribution network.

Test system modified with addition 2 DGs connected at buses number 5 and 7 with power equals 5MVA and power factor nominally is 0.9 lagging and their type are synchronous. This modification is from [45] and 3 phase short circuit currents at both near-end and far-end from [38].

The current transformer's ratios of relays are 120, 120, 120, 40, 120, 40, 120, 120, 120, 80, 80, 80, 40, 40, 80, and 80, for relays from 1 to 16, respectively [38].

In this test system, optimization algorithms tuned 48 variables that are limited by minimum and maximum values. Then constrained between operation time values of relays by CTI. This test system is more constrained than the previous test system by 41 between primary and backup DOCRs and 44 between DOCRs and distance relays, in both ends (near and far).

Optimal settings tuned by SBO and MSBO algorithms. Those were tabulated in Table 4 for the normal case and another case. These optimization solutions passed CTI constraints between relays pairs in normal case in Table 5. Then, Table 6 proved the ability of optimization solutions to pass the CTI constraint between relays pairs in DGs working case.

Figure 12 shows the convergence characteristics curve of both SBO and MSBO algorithms in the normal case while in another case after DGs work is shown in Figure 13. During the tuning process for relays setting by optimization algorithms SBO and MSBO, the penalty of both are shown in Figures 14 and 15 for the normal case and the other DGs case, respectively.

In the normal case, MSBO has OF with a value of 34.806 s and is better than SBO with 2.05 s. MSBO reached 36.860 s faster than SBO by 328 iterations and passed penalty after 22 iterations the original SBO passed after 71 iterations. In another case, MSBO reaches SBO's OF after 482 iterations and at the end of the run reaches 51.068 s as OF and better than SBO by 6.2 s. MSBO passed constraints penalty after 113 iterations while SBO still penalty to 183 iterations.

Table 4. IEEE 14-bus distribution network's relays setting.

Relay	Normal Topological						With External DG					
	Original SBO			Modified SBO			Original SBO			Modified SBO		
	TDS	IP	TZ2	TDS	IP	TZ2	TDS	IP	TZ2	TDS	IP	TZ2
1	0.223	235.93	1.246	0.214	157.86	0.984	0.386	392.93	1.549	0.384	337.37	1.442
2	0.11	185.11	0.885	0.159	149.46	1.028	0.37	188.60	1.455	0.209	314.56	1.153
3	0.135	232.94	0.931	0.155	164.17	0.858	0.434	139.04	1.255	0.241	465.02	1.243
4	0.156	51.91	1.103	0.232	20.02	0.937	0.376	52.32	1.455	0.402	39.28	1.376
5	0.243	80.15	0.824	0.211	142.21	0.895	0.492	231.73	1.514	0.289	394.61	1.18
6	0.361	28.91	1.069	0.219	63.82	0.937	0.356	131.99	1.454	0.621	28.58	1.407
7	0.241	140.62	0.865	0.164	425.78	1.025	0.731	71.12	1.446	0.33	361.09	1.172
8	0.258	60.58	0.953	0.15	117.13	0.815	0.447	106.48	1.367	0.283	233.98	1.266
9	0.105	308.66	0.864	0.162	197.06	0.923	0.349	347.18	1.423	0.363	260.94	1.308
10	0.121	187.97	1.162	0.116	167.35	1.014	0.311	239.60	1.566	0.447	72.25	1.299
11	0.158	176.02	0.854	0.282	85.18	1.008	0.529	119.67	1.414	0.324	209.62	1.121
12	0.229	150.99	1.294	0.165	133.91	0.93	0.534	105.85	1.499	0.569	69.66	1.398
13	0.151	101.59	1.077	0.185	58.68	0.929	0.399	85.44	1.345	0.464	60.89	1.362
14	0.205	65.11	0.8	0.313	27.29	0.861	0.46	54.40	1.088	0.444	58.67	1.078
15	0.136	179.69	0.953	0.139	152.58	0.878	0.489	106.17	1.38	0.298	276.49	1.297
16	0.119	201.72	1.092	0.198	89.52	0.984	0.491	102.67	1.494	0.4	141.69	1.408
OF		36.86			34.806			57.268			51.068	

Table 5. IEEE 14-bus distribution network's operation times of Relay's pairs in normal case by MSBO.

Pair	Near-End						Far-End					
	DOCRs			D&DOCR			DOCRs			D&DOCR		
	T_p	T_b	CTI	T_p	T_{Z2B}	CTI′	T_p	T_b	CTI	T_p	T_{Z2P}	CTI′
1	0.537	0.737	0.201	0.537	0.937	0.401	0.784	1.096	0.312	0.784	0.984	0.2
2	0.537	0.737	0.201	0.537	0.937	0.401	0.784	1.272	0.488	0.784	0.984	0.2
3	0.575	0.808	0.233	0.575	1.008	0.433	0.828	1.032	0.203	0.828	1.028	0.2
4	0.374	0.828	0.455	0.374	1.028	0.655	0.658	1.997	1.339	0.658	0.858	0.2
5	0.374	0.737	0.364	0.374	0.937	0.564	0.658	——	——	0.658	0.858	0.2
6	0.427	0.661	0.234	0.427	0.861	0.434	0.737	1.907	1.169	0.737	0.937	0.2
7	0.504	0.828	0.325	0.504	1.028	0.525	0.695	1.352	0.657	0.695	0.895	0.2
8	0.504	0.737	0.234	0.504	0.937	0.434	0.695	——	——	0.695	0.895	0.2
9	0.524	0.729	0.204	0.524	0.929	0.404	0.737	——	——	0.737	0.937	0.2
10	0.524	0.784	0.259	0.524	0.984	0.459	0.737	0.938	0.201	0.737	0.937	0.2
11	0.613	0.814	0.2	0.613	1.014	0.4	0.825	1.546	0.721	0.825	1.025	0.2
12	0.529	0.73	0.201	0.529	0.93	0.401	0.615	0.856	0.241	0.615	0.815	0.2
13	0.413	0.615	0.202	0.413	0.815	0.402	0.723	7.393	6.669	0.723	0.923	0.2
14	0.476	0.676	0.2	0.476	0.878	0.403	0.814	1.703	0.89	0.814	1.014	0.2
15	0.621	0.825	0.204	0.621	1.025	0.404	0.808	1.604	0.796	0.808	1.008	0.2
16	0.54	0.784	0.244	0.54	0.984	0.444	0.73	1.066	0.336	0.73	0.93	0.2
17	0.452	0.658	0.205	0.452	0.858	0.405	0.729	2.547	1.819	0.729	0.929	0.2
18	0.495	0.695	0.2	0.495	0.895	0.4	0.661	2.583	1.922	0.661	0.861	0.2
19	0.495	0.784	0.289	0.495	0.984	0.489	0.661	1.187	0.526	0.661	0.861	0.2
20	0.391	0.695	0.304	0.391	0.895	0.504	0.678	1.445	0.766	0.678	0.878	0.2
21	0.391	0.729	0.337	0.391	0.929	0.537	0.678	1.66	0.982	0.678	0.878	0.2
22	0.522	0.723	0.201	0.522	0.923	0.401	0.784	1.886	1.102	0.784	0.984	0.2

Table 6. IEEE 14-bus distribution network's operation times of relays pairs with DGs by MSBO.

Pair	Near-End						Far-End					
	DOCRs			D&DOCR			DOCRs			D&DOCR		
	T_p	T_b	CTI	T_p	T_{Z2B}	CTI	T_p	T_b	CTI	T_p	T_{Z2P}	CTI
1	0.973	1.18	0.207	0.973	1.376	0.403	1.242	1.871	0.629	1.242	1.442	0.2
2	0.973	1.205	0.232	0.973	1.407	0.434	1.242	2.081	0.839	1.242	1.442	0.2
3	0.718	0.921	0.203	0.718	1.121	0.403	0.953	1.159	0.207	0.953	1.153	0.2
4	0.644	0.956	0.312	0.644	1.153	0.509	1.043	1.508	0.464	1.043	1.243	0.2
5	0.644	1.205	0.562	0.644	1.407	0.763	1.043	——	——	1.043	1.243	0.2
6	0.677	0.881	0.204	0.677	1.078	0.401	1.176	26.389	25.213	1.176	1.376	0.2
7	0.752	0.956	0.204	0.752	1.153	0.401	0.98	1.506	0.525	0.98	1.18	0.2
8	0.752	1.18	0.428	0.752	1.376	0.624	0.98	——	——	0.98	1.18	0.2
9	0.948	1.162	0.214	0.948	1.362	0.414	1.207	——	——	1.207	1.407	0.2
10	0.948	1.206	0.258	0.948	1.408	0.46	1.207	1.409	0.202	1.207	1.407	0.2
11	0.873	1.1	0.227	0.873	1.299	0.427	0.972	1.323	0.351	0.972	1.172	0.2
12	0.947	1.181	0.234	0.947	1.398	0.451	1.066	1.271	0.205	1.066	1.266	0.2
13	0.832	1.059	0.227	0.832	1.266	0.433	1.108	3.803	2.695	1.108	1.308	0.2
14	0.892	1.097	0.205	0.892	1.297	0.405	1.099	1.821	0.722	1.099	1.299	0.2
15	0.768	0.972	0.204	0.768	1.172	0.404	0.921	1.22	0.299	0.921	1.121	0.2
16	1.038	1.242	0.204	1.038	1.442	0.404	1.198	1.611	0.413	1.198	1.398	0.2
17	0.826	1.032	0.206	0.826	1.243	0.417	1.162	6.046	4.884	1.162	1.362	0.2
18	0.691	0.98	0.29	0.691	1.18	0.49	0.878	2.43	1.553	0.878	1.078	0.2
19	0.691	1.206	0.515	0.691	1.408	0.717	0.878	1.489	0.612	0.878	1.078	0.2
20	0.766	0.98	0.215	0.766	1.18	0.415	1.097	1.637	0.54	1.097	1.297	0.2
21	0.766	1.162	0.397	0.766	1.362	0.597	1.097	1.603	0.506	1.097	1.297	0.2
22	0.908	1.108	0.2	0.908	1.308	0.4	1.208	1.735	0.527	1.208	1.408	0.2

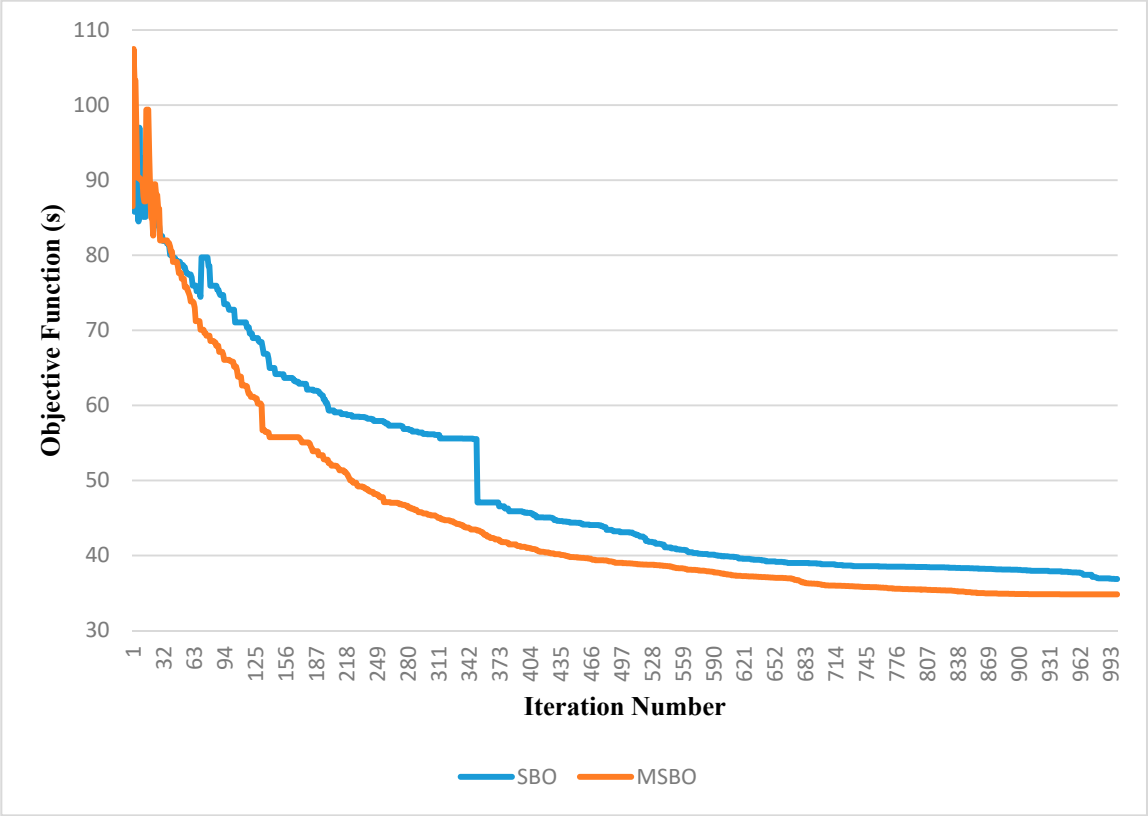

Figure 12. Convergence characteristics of SBO and MSBO in normal case of IEEE 14-bus distribution network.

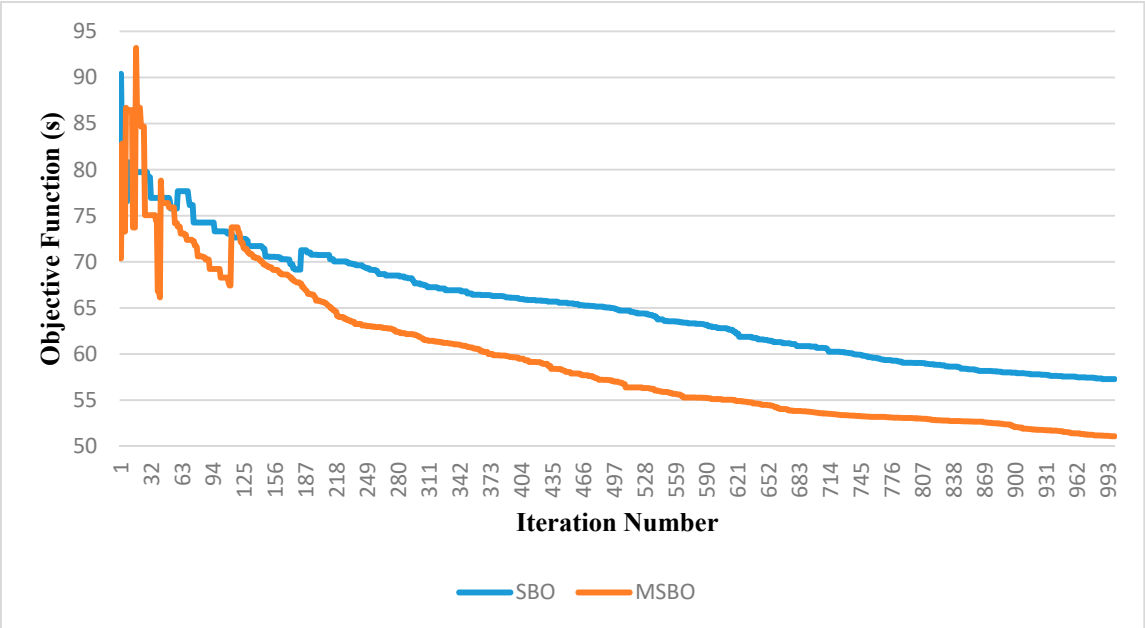

Figure 13. Convergence characteristics of SBO and MSBO with DGs case of IEEE 14-bus distribution network.

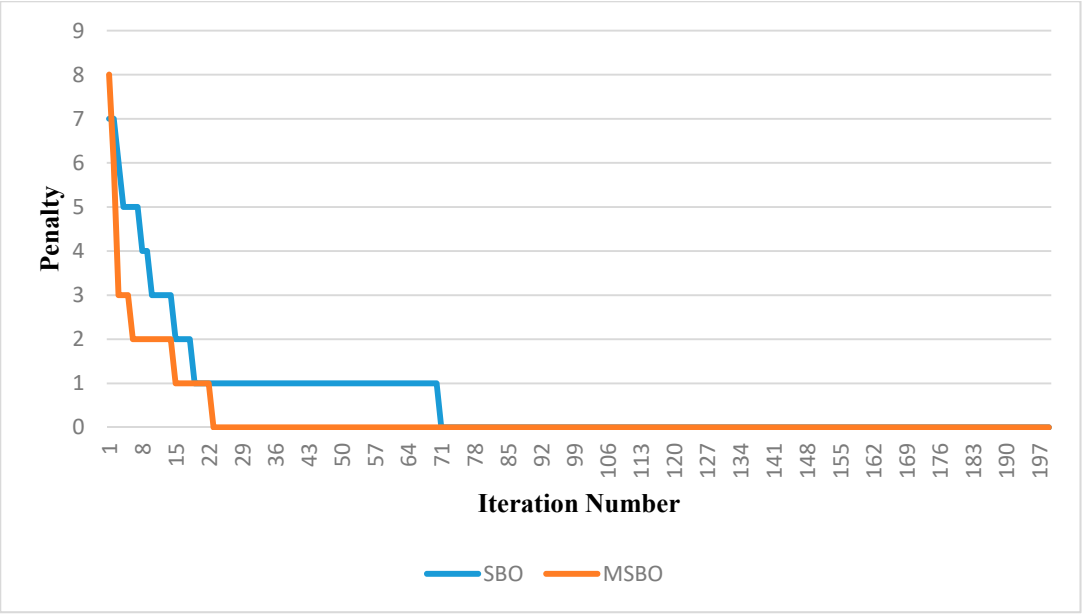

Figure 14. Penalty between SBO and MSBO of IEEE 14-bus distribution network normal case.

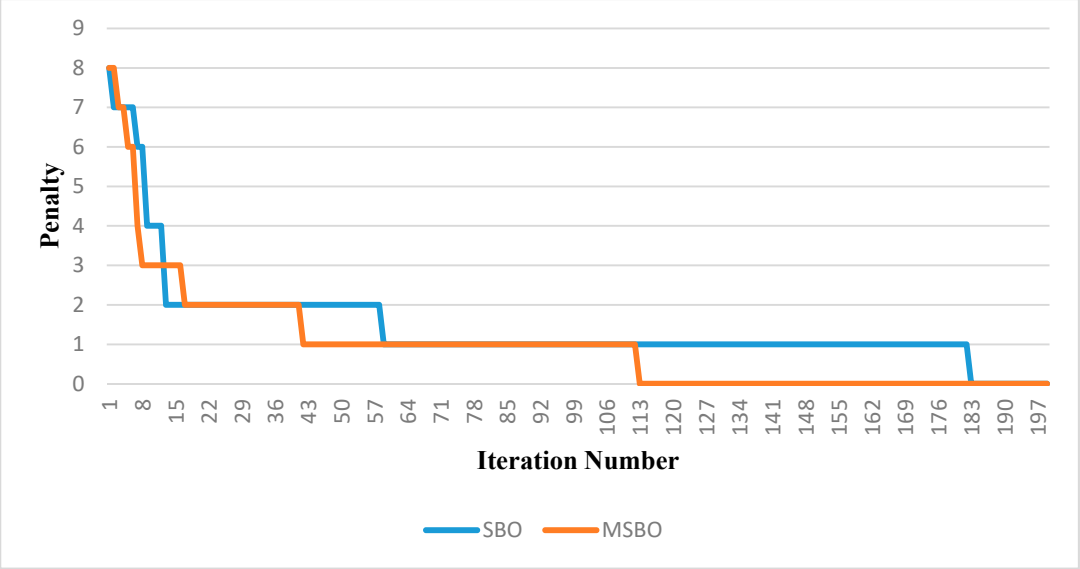

Figure 15. Penalty between SBO and MSBO of IEEE 14-bus distribution network with DGs.

4.3. Varification of MSBO Using Etap 12.6.0

Etap is used to verify the results obtained by the proposed algorithm MSBO on 8 bus normal grid, three-phase fault at transmission line between third and fourth bus-bars. This fault applied in both the near end and far end. As simulation by Etap as shown in Figure 16. Relay 3 is the primary relay that operates at 0.535 s and 0.615 s in the near and far end, respectively. While relay 2 is its backup relay which operates at 0.736 s and 0.943 in near and far ends, respectively. And these verify the CTI is more than or equal to 0.2 s and DOCRs without miscoordination. That simulation is also done at the transmission line between the fifth and sixth busbars additional to relays 5 as primary relay and 4 as backup re-lay, the operation time at both ends near and far of this pair relay as 0.318 s, 0.519 s, 0.717 s, and 1.738 s, respectively. The simulation is presented in Figure 17 proved that there is no miscoordination between DOCRs.

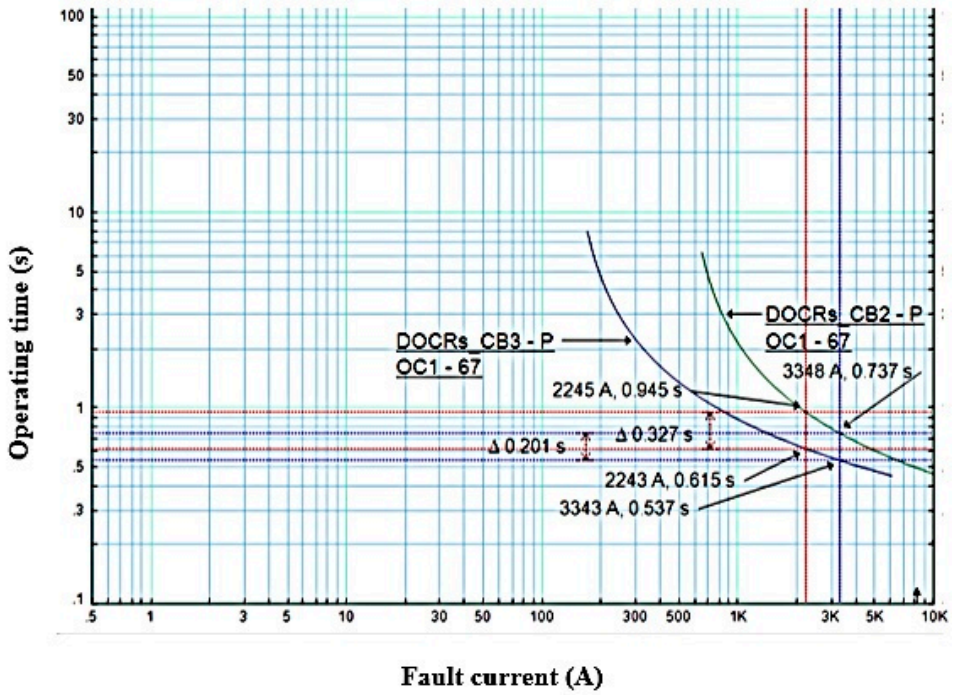

Figure 16. Operating times for relays 3 and 2.

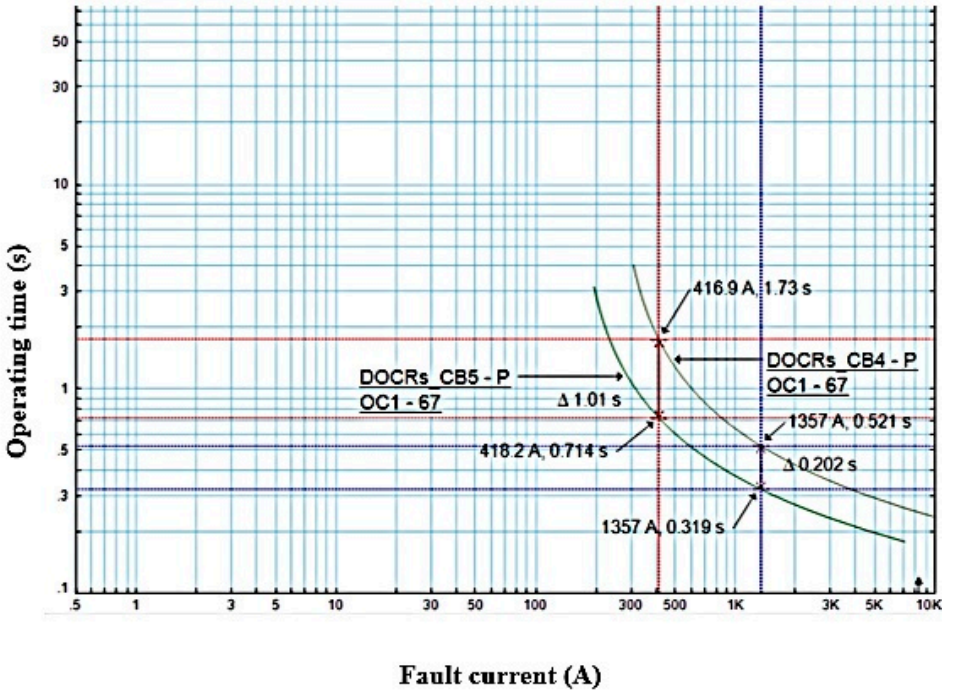

Figure 17. Operating times for relays 5 and 4.

Finally, simulation is done at the transmission line which is connected between the first and third busbars. It is noticed from Figure 18. Operating times at the near end for primary (relay 9), and backup (relay 10) are 0.298 s, and 0.498 s, respectively. At the far end the operating time of primary and backup relays are 0.661 s, and 1.216 s, respectively. This case avoids miscoordination too.

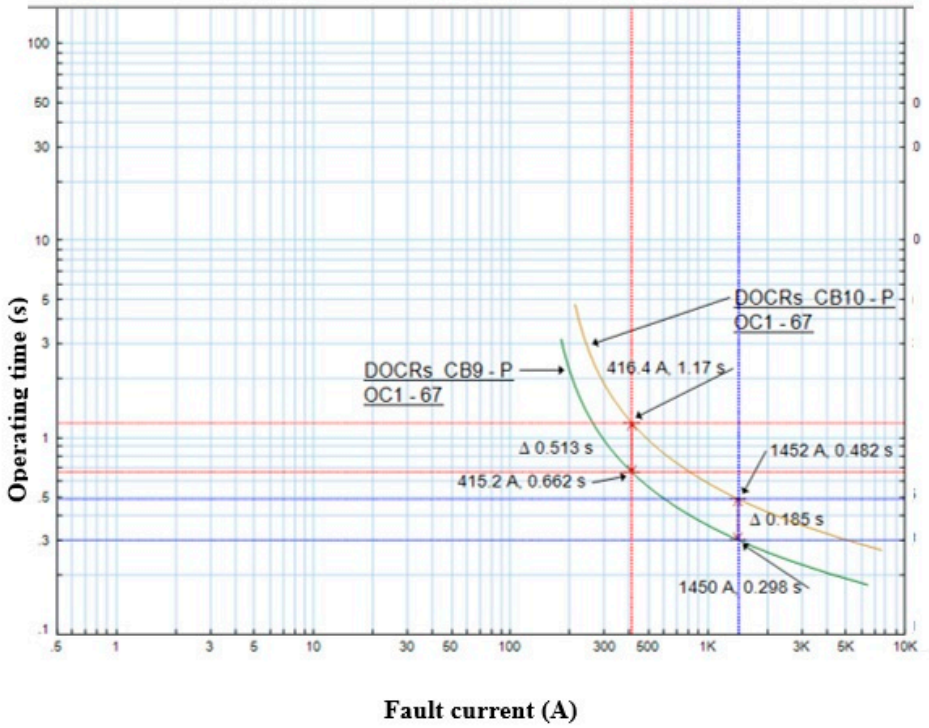

Figure 18. Operating times for relays 9 and 10.

5. Conclusions

In this research work, the APS passed the miscoordination problem between primary and backup DOCRs, as well as miscoordination between DOCRs and distance relays. The results demonstrated that APS has the potential to coordinate protection relays with appropriate settings to face the problem of DGs in the distribution network. Without miscoordination between protection relays, the power system can investigate the advantages of both distance relays and DOCRs. In addition to the role of the modified optimization algorithm, which improved the optimal values and reduced operation relay's time, all operation times of both primary DOCRs and distance second zone's time were set below the maximum operation time. The modified algorithm has better convergence characteristics and achieves better optimal values with fewer iterations.

Author Contributions: Conceptualization, S.K. and A.K.; Data curation, S.K. and A.K.; formal analysis, S.K., A.K., M.T.-V., F.A.B. and M.I.M.; funding acquisition, F.A.B. and M.I.M.; investigation, M.A., S.K., A.K. and M.T.-V.; methodology, M.A., S.K. and A.K.; project administration, S.K., M.T.-V., F.A.B. and M.I.M.; resources, S.K. and M.T.-V.; software, S.K.; supervision, S.K., A.K., M.T.-V., F.A.B. and M.I.M.; validation, M.A., S.K. and A.K.; visualization, M.T.-V., F.A.B. and M.I.M.; writing—original draft, M.A. and A.K.; writing—review & editing, S.K. and M.T.-V. All authors have read and agreed to the published version of the manuscript.

Funding: The authors thank the support of the National Research and Development Agency of Chile (ANID), ANID/Fondap/15110019.

Institutional Review Board Statement: Not applicable.

Informed Consent Statement: Not applicable.

Data Availability Statement: Not applicable.

Conflicts of Interest: The authors declare no conflict of interest.

Appendix A

Table A1. Three-phase short circuit currents for IEEE 8-bus in the normal case by ETAP in both near end and far end.

Pair	Primary Relay	Back-Up Relay	Near-End		Far-End	
			Primary	Back-Up	Primary	Back-Up
1	1	6	2703	2703	812	812
2	2	1	5390	812	3347	309
3	2	7	5390	1540	3347	586
4	3	2	3347	3347	2243	2243
5	4	3	2243	2243	1361	1361
6	5	4	1361	1361	416	416
7	6	5	4995	416	2703	20
8	6	14	4995	1540	2703	72
9	7	5	4267	416	1540	REV
10	7	13	4267	812	1540	REV
11	8	7	4995	1540	2507	REV
12	8	9	4995	416	2507	REV
13	9	10	1453	1453	416	416
14	10	11	2344	2344	1453	1453
15	11	12	3495	3495	2344	2344
16	12	13	5390	812	3495	348
17	12	14	5390	1540	3495	661
18	13	8	2507	2507	812	812
19	14	1	4267	812	1540	REV
20	14	9	4267	416	1540	REV

References

1. Abdelhamid, M.; Kamel, S.; Mohamed, M.A.; Aljohani, M.; Rahmann, C.; Mosaad, M.I. Political Optimization Algorithm for Optimal Coordination of Directional Overcurrent Relays. In Proceedings of the 2020 IEEE Electric Power and Energy Conference (EPEC), Edmonton, AB, Canada, 9–10 November 2020; pp. 1–7. [CrossRef]
2. Damchi, Y.; Sadeh, J.; Mashhadi, H.R. Considering pilot protection in the optimal coordination of distance and directional overcurrent relays. *Iran. J. Electr. Electron. Eng.* **2015**, *11*, 154–164.
3. Perez, L.G.; Urdaneta, A.J. Optimal computation of distance relays second zone timing in a mixed protection scheme with directional overcurrent relays. *IEEE Trans. Power Deliv.* **2001**, *16*, 385–388. [CrossRef]
4. Khederzadeh, M. Back-up protection of distance relay second zone by directional overcurrent relays with combined curves. In Proceedings of the 2006 IEEE Power Engineering Society General Meeting, Montreal, QC, Canada, 18–22 June 2006; p. 6. [CrossRef]
5. Sarwagya, K.; Nayak, P.K.; Ranjan, S. Optimal coordination of directional overcurrent relays in complex distribution networks using sine cosine algorithm. *Electr. Power Syst. Res.* **2020**, *187*, 106435. [CrossRef]
6. Ates, Y.; Uzunoglu, M.; Karakas, A.; Boynuegri, A.R.; Nadar, A.; Dag, B. Implementation of adaptive relay coordination in distribution systems including distributed generation. *J. Clean. Prod.* **2016**, *112*, 2697–2705. [CrossRef]
7. Akdag, O.; Yeroglu, C. Optimal directional overcurrent relay coordination using MRFO algorithm: A case study of adaptive protection of the distribution network of the Hatay province of Turkey. *Electr. Power Syst. Res.* **2021**, *192*, 106998. [CrossRef]
8. Mansour, M.M.; Mekhamer, S.F.; El-Kharbawe, N. A modified particle swarm optimizer for the coordination of directional overcurrent relays. *IEEE Trans. Power Deliv.* **2007**, *22*, 1400–1410. [CrossRef]
9. Noghabi, A.S.; Sadeh, J.; Mashhadi, H.R. Considering different network topologies in optimal overcurrent relay coordination using a hybrid GA. *IEEE Trans. Power Deliv.* **2009**, *24*, 1857–1863. [CrossRef]
10. Albasri, F.A.; Alroomi, A.R.; Talaq, J.H. Optimal coordination of directional overcurrent relays using biogeography-based optimization algorithms. *IEEE Trans. Power Deliv.* **2015**, *30*, 1810–1820. [CrossRef]
11. Shih, M.Y.; Enriquez, A.C. Novel coordination of DOCRs using trigonometric differential evolution algorithm. *IEEE Lat. Am. Trans.* **2015**, *13*, 1605–1611. [CrossRef]
12. Khurshaid, T.; Wadood, A.; Farkoush, S.G.; Kim, C.-H.; Yu, J.; Rhee, S.-B. Improved firefly algorithm for the optimal coordination of directional overcurrent relays. *IEEE Access* **2019**, *7*, 78503–78514. [CrossRef]
13. Khurshaid, T.; Wadood, A.; Farkoush, S.G.; Yu, J.; Kim, C.-H.; Rhee, S.-B. An improved optimal solution for the directional overcurrent relays coordination using hybridized whale optimization algorithm in complex power systems. *IEEE Access* **2019**, *7*, 90418–90435. [CrossRef]

14. Yu, J.; Kim, C.-H.; Rhee, S.-B. Oppositional jaya algorithm with distance-adaptive coefficient in solving directional over current relays coordination problem. *IEEE Access* **2019**, *7*, 150729–150742. [CrossRef]
15. Korashy, A.; Kamel, S.; Alquthami, T.; Jurado, F. Optimal coordination of standard and non-standard direction overcurrent relays using an improved moth-flame optimization. *IEEE Access* **2020**, *8*, 87378–87392. [CrossRef]
16. Abdelhamid, M.; Kamel, S.; Mohamed, M.A.; Rahmann, C. An Effective Approach for Optimal Coordination of Directional Overcurrent Relays Based on Artificial Ecosystem Optimizer. In Proceedings of the 2021 IEEE International Conference on Automation/XXIV Congress of the Chilean Association of Automatic Control (ICA-ACCA), Valparaíso, Chile, 22–26 March 2021; pp. 1–6. [CrossRef]
17. Korashy, A.; Kamel, S.; Houssein, E.H.; Jurado, F.; Hashim, F.A. Development and application of evaporation rate water cycle algorithm for optimal coordination of directional overcurrent relays. *Expert Syst. Appl.* **2021**, *185*, 115538. [CrossRef]
18. Marcolino, M.H.; Leite, J.B.; Mantovani, J.R.S. Optimal coordination of overcurrent directional and distance relays in meshed networks using genetic algorithm. *IEEE Lat. Am. Trans.* **2015**, *13*, 2975–2982. [CrossRef]
19. Tiwari, R.; Singh, R.K.; Choudhary, N.K. A Comparative Analysis of Optimal Coordination of Distance and Overcurrent Relays with Standard Relay Characteristics using GA, GWO and WCA. In Proceedings of the 2020 IEEE Students Conference on Engineering & Systems (SCES), Prayagraj, India, 10–12 July 2020; pp. 1–6.
20. Bangar, P.A.; Kalage, A.A. Optimum coordination of overcurrent and distance relays using JAYA optimization algorithm. In Proceedings of the 2017 International Conference on Nascent Technologies in Engineering (ICNTE), Vashi, India, 27–28 January 2017; pp. 1–5.
21. Rivas, A.E.L.; Pareja, L.A.G.; Abrão, T. Coordination of distance and directional overcurrent relays using an extended continuous domain ACO algorithm and an hybrid ACO algorithm. *Electr. Power Syst. Res.* **2019**, *170*, 259–272. [CrossRef]
22. Vijayakumar, D.; Nema, R.K. A novel optimal setting for directional over current relay coordination using particle swarm optimization. *Int. J. Electr. Power Energy Syst. Eng.* **2008**, *1*, 82.
23. Singh, D.K.; Gupta, S. Optimal coordination of directional overcurrent relays: A genetic algorithm approach. In Proceedings of the 2012 IEEE Students' Conference on Electrical, Electronics and Computer Science, Bhopal, India, 1–2 March 2012; pp. 1–4.
24. Moirangthem, J.; Krishnanand, K.R.; Dash, S.S.; Ramaswami, R. Adaptive differential evolution algorithm for solving non-linear coordination problem of directional overcurrent relays. *IET Gener. Transm. Distrib.* **2013**, *7*, 329–336. [CrossRef]
25. Shih, M.Y.; Salazar, C.A.C.; Enríquez, A.C. Adaptive directional overcurrent relay coordination using ant colony optimization. *IET Gener. Transm. Distrib.* **2015**, *9*, 2040–2049. [CrossRef]
26. Chawla, A.; Bhalja, B.R.; Panigrahi, B.K.; Singh, M. Gravitational search based algorithm for optimal coordination of directional overcurrent relays using user defined characteristic. *Electr. Power Compon. Syst.* **2018**, *46*, 43–55. [CrossRef]
27. Tjahjono, A.; Anggriawan, D.O.; Faizin, A.K.; Priyadi, A.; Pujiantara, M.; Taufik, T.; Purnomo, M.H. Adaptive modified firefly algorithm for optimal coordination of overcurrent relays. *IET Gener. Transm. Distrib.* **2017**, *11*, 2575–2585. [CrossRef]
28. ElSayed, S.K.; Elattar, E.E. Hybrid Harris hawks optimization with sequential quadratic programming for optimal coordination of directional overcurrent relays incorporating distributed generation. *Alex. Eng. J.* **2021**, *60*, 2421–2433. [CrossRef]
29. Farshchin, M.; Maniat, M.; Camp, C.V.; Pezeshk, S. School based optimization algorithm for design of steel frames. *Eng. Struct.* **2018**, *171*, 326–335. [CrossRef]
30. Rao, R.V.; Savsani, V.J.; Vakharia, D.P. Teaching–learning-based optimization: A novel method for constrained mechanical design optimization problems. *Comput. Aided Des.* **2011**, *43*, 303–315. [CrossRef]
31. Degertekin, S.O.; Tutar, H.; Lamberti, L. School-based optimization for performance-based optimum seismic design of steel frames. *Eng. Comput.* **2021**, *37*, 3283–3297. [CrossRef]
32. Abdelghany, R.Y.; Kamel, S.; Ramadan, A.; Sultan, H.M.; Rahmann, C. Solar Cell Parameter Estimation Using School-Based Optimization Algorithm. In Proceedings of the 2021 IEEE International Conference on Automation/XXIV Congress of the Chilean Association of Automatic Control (ICA-ACCA), Valparaíso, Chile, 22–26 March 2021; pp. 1–6. [CrossRef]
33. Sampaio, F.C.; Leão, R.P.S.; Sampaio, R.F.; Melo, L.S.; Barroso, G.C. A multi-agent-based integrated self-healing and adaptive protection system for power distribution systems with distributed generation. *Electr. Power Syst. Res.* **2020**, *188*, 106525. [CrossRef]
34. Reis, F.B.d.; Pinto, J.O.C.P.; Reis, F.S.d.; Issicaba, D.; Rolim, J.G. Multi-agent dual strategy based adaptive protection for microgrids. *Sustain. Energy Grids Netw.* **2021**, *27*, 100501. [CrossRef]
35. Cui, Q.; Weng, Y. An environment-adaptive protection scheme with long-term reward for distribution networks. *Int. J. Electr. Power Energy Syst.* **2020**, *124*, 106350. [CrossRef]
36. Elmitwally, A.; Kandil, M.S.; Gouda, E.; Amer, A. Mitigation of DGs impact on variable-topology meshed network protection system by optimal fault current limiters considering overcurrent relay coordination. *Electr. Power Syst. Res.* **2020**, *186*, 106417. [CrossRef]
37. Yazdaninejadi, A.; Nazarpour, D.; Golshannavaz, S. Sustainable electrification in critical infrastructure: Variable characteristics for overcurrent protection considering DG stability. *Sustain. Cities Soc.* **2020**, *54*, 102022. [CrossRef]
38. Rajput, V.N.; Adelnia, F.; Pandya, K.S. Optimal coordination of directional overcurrent relays using improved mathematical formulation. *IET Gener. Transm. Distrib.* **2018**, *12*, 2086–2094. [CrossRef]
39. Moravej, Z.; Ooreh, O.S. Coordination of distance and directional overcurrent relays using a new algorithm: Grey wolf optimizer. *Turk. J. Electr. Eng. Comput. Sci.* **2018**, *26*, 3130–3144. [CrossRef]

40. Mohammadi, R.; Abyaneh, H.A.; Rudsari, H.M.; Fathi, S.H.; Rastegar, H. Overcurrent relays coordination considering the priority of constraints. *IEEE Trans. Power Deliv.* **2011**, *26*, 1927–1938. [CrossRef]
41. Shih, M.Y.; Conde, A.; Ángeles-Camacho, C.; Fernández, E.; Leonowicz, Z.; Lezama, F.; Chan, J. A two stage fault current limiter and directional overcurrent relay optimization for adaptive protection resetting using differential evolution multi-objective algorithm in presence of distributed generation. *Electr. Power Syst. Res.* **2021**, *190*, 106844. [CrossRef]
42. Camp, C.V.; Farshchin, M. Design of space trusses using modified teaching-learning based optimization. *Eng. Struct.* **2014**, *62*, 87–97. [CrossRef]
43. Yang, M.-T.; Liu, A. Applying hybrid PSO to optimize directional overcurrent relay coordination in variable network topologies. *J. Appl. Math.* **2013**, *2013*, 879078. [CrossRef]
44. Christie, R. Power systems test case archive. *Electr. Eng. Dept. Univ. Wash.* **2000**, *108*. Available online: https://labs.ece.uw.edu/pstca/ (accessed on 10 October 2021).
45. Saleh, K.A.; Zeineldin, H.H.; Al-Hinai, A.; El-Saadany, E.F. Optimal coordination of directional overcurrent relays using a new time-current-voltage characteristic. *IEEE Trans. Power Deliv.* **2014**, *30*, 537–544. [CrossRef]